Proceedings of Building Simulation 2011:
12th Conference of International Building Performance Simulation Association, Sydney, 14-16 November.

FUNDAMENTAL NUMERICAL ANALYSIS OF INSOLATION OF THE HUMAN BODY

Koji Sakai[1], Taku Ito[1], Hiroki Ono[1], Ryoichi Kajiya[1] and Toshihiko Sudo[2]
[1]School of Science & Technology, Meiji University, Kawasaki, Japan
[2]Nikken Sekkei Research Institute, Tokyo, Japan

ABSTRACT

Uneven thermal environments often result from insolation or radiation in outdoor spaces and half outdoor spaces such as arcades and under open membrane roofs. Similar environments are observed in the perimeter spaces of office buildings in winter during the daytime. To estimate thermal environments in such spaces, detailed consideration must be given to the effects of both insolation and long-wavelength radiation on each part of the human body. This study conducted fundamental analysis of the calculations of insolation of a human body. The incident insolation to each part of a human body was evaluated. The results are reported herein.

INTRODUCTION

Uneven thermal environments are often caused by insolation or radiation in outdoor spaces and half-outdoor spaces such as arcades and under open membrane roofs. Similarly, perimeter spaces are penetrated by insolation. Detailed consideration must be devoted to effects of both insolation and long-wavelength radiation on each part of a human body to estimate thermal environments in such spaces. Insolation and radiation into a human body outdoors are classified into direct solar radiation (Direct), diffuse sky radiation (Diffuse), reflected solar radiation (Reflect), and atmospheric radiation and ground surface radiation (Long wave), as presented in Fig. 1. Each term demands specific computation. Some examples are that the projected area of a human body to the solar position direction is necessary for computation of direct solar radiation, although the shape factor of a human body to the sky is necessary for the computation of diffuse sky radiation and atmospheric radiation. Moreover, computation of the reflected solar radiation and ground surface radiation from features demands the estimation of the shape factor of a human body to them in advance.

Studies of evaluation of the projected area and effective radiation area of a human body include direct measurements from a human body by Underwood (Underwood et al., 1966) and Fanger (Fanger et al., 1970), and a procedure using a numerical human body by Ozeki (Ozeki et al., 1999). In the meantime, Pickup (Pickup et al., 1999)

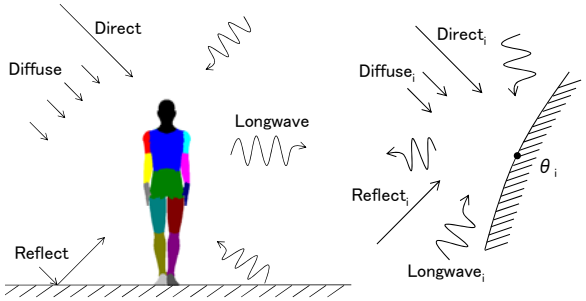

Fig. 1 Outdoor radiation environment model.

proposed OUT_MRT, which converts all radiant heat into a mean radiant temperature, as a procedure for estimating insolation of a human body. However, these procedures treat only the effects of insolation and radiation on a human body as a whole. They do not address the effects on each part of a human body, such as a hand, a leg, or the chest. A 65-division thermoregulation numerical human body model simulating a variable skin temperature thermal mannequin has been proposed for the thermal comfort evaluation of a human body, which allows evaluation of an uneven thermal environment. This study produced a procedure for computing incident solar radiation to each human body part. The procedure is applicable to a 65-division thermoregulation numerical human body model based on the methods presented by Ozeki et al. and Pickup et al. Then incident insolation to each part of a human body was evaluated. The results are reported herein.

OUT_MRT (Review of the study by Pickup et al.)

OUT_MRT by Pickup is one index used to evaluate the outdoor solar radiation environment. Normal direct solar radiation (J_{DN} [W/m^2]), horizontal diffuse sky radiation (J_{SH} [W/m^2]), atmospheric radiation (J_a [W/m^2]), and ground surface radiation (J_g [W/m^2]) are assumed as known, and insolation and radiation balance for a human body surface are considered. Letting the orthographic projection area of a human body to the insolation direction be A_p [m^2], and letting the projected area rate to human body surface area (A_{DU} [m^2]) be $f_p = A_p/A_{DU}$ [–], then direct solar radiation absorbed by a human body is given as

$$Direct = f_p(1 - a_{body})J_{DN} \quad (1)$$

where a_{body} is the solar reflectance of the whole human body and f_p is dependent on the solar position and human body contour. Pickup adopted the following equation as an approximate formula for f_p (where β is solar altitude):

$$f_p = 0.42\cos\beta + 0.043\sin\beta \quad (2)$$

Next, diffuse sky radiation into a human body is given as

$$Diffuse = E_{ff}^{U}(1-a_{body})J_{SH} \quad (3)$$

Therein, E_{ff}^{U} corresponds to the shape factor of a human body to the sky. The effective radiation area rate over the upper hemisphere of the whole global region surrounding a human body is as described below; it is dependent on the human body contour.

Reflected solar radiation from the ground surface onto a human body (perfect diffusion) is expressed as

$$Reflect = E_{ff}^{D}(1-a_{body})(J_{DH}+J_{SH})a_{grd} \quad (4)$$

where E_{ff}^{D} signifies the effective radiation area rate to the lower hemisphere, a_{grd} stands for the solar reflectance of earth surface, and $J_{DH} = J_{DN}\sin\beta$.

Long-wavelength radiation transfer on a human body surface is obtained as

$$\begin{aligned} Longwave &= E_{ff}^{U}(J_a - \varepsilon_{body}\sigma T_{body}^4) + E_{ff}^{D}(J_g - \varepsilon_{body}\sigma T_{body}^4) \\ &= E_{ff}^{U}J_a + E_{ff}^{D}J_g - E_{ff}\cdot\varepsilon_{body}\sigma T_{body}^4 \end{aligned} \quad (5)$$

where $E_{ff} = E_{ff}^{U} + E_{ff}^{D}$ represents the global effective radiation area rate, ε_{body} signifies the long-wavelength radiation rate of the whole human body, T_{body} denotes the human body surface temperature [K], and σ is the Stefan–Boltzmann's constant. The sum of Eqs. (1), (3)–(5) is the total global radiation transfer received by a human body.

The radiation transfer of a human body in its surrounding closed volume with uniform surface temperature at T_{MRT} is given as

$$FLUX\_ENC = E_{ff}\sigma(\varepsilon_{ENC}T_{MRT}^4 - \varepsilon_{body}T_{body}^4) \quad (6)$$

where ε_{ENC} is the emissivity of surrounding closed volume assumed as a perfectly black body.

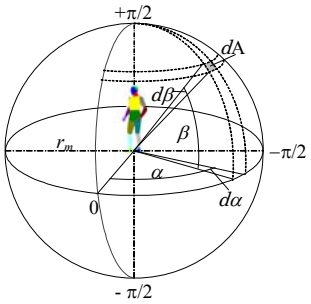

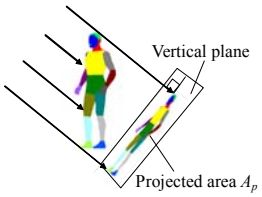

A human body standing at the origin was subjected to a rotation matrix about Z-axis (azimuth, β) and X-axis (altitude, α), then drawn.

Fig.2Enclosed region and Projection for parallel ray

A thermal equilibrium equation is derived from the sum of Equations (1), (3)–(5) and (6) as

$$\begin{aligned} &E_{ff}\sigma(T_{MRT}^4 - \varepsilon_{body}T_{body}^4) \\ &= Longwave + Direct + Diffuse + Reflect \end{aligned} \quad (7)$$

Consequently, T_{MRT} is derived from above as

$$\begin{aligned} T_{MRT} = \Bigg[&\frac{E_{ff}^{U}}{\sigma E_{ff}}J_a + \frac{E_{ff}^{D}}{\sigma E_{ff}}J_g \\ &+ \frac{f_p(1-a_{body})}{\sigma E_{ff}}J_{DN} + \frac{E_{ff}^{U}}{\sigma E_{ff}}(1-a_{body})J_{SH} \\ &+ \frac{E_{ff}^{D}}{\sigma E_{ff}}(1-a_{body})(J_{DH}+J_{SH})\cdot a_{gnd} \Bigg]^{0.25} \end{aligned} \quad (8)$$

which is further simplified with $E_{ff}^{U} = E_{ff}^{D} = E_{ff}/2$ as

$$\begin{aligned} T_{MRT} = \Bigg[&\frac{1}{2\sigma}(J_a + J_g) + \frac{f_p(1-a_{body})}{\sigma E_{ff}}J_{DN} \\ &+ \frac{(1-a_{body})}{2\sigma}(J_{SH} + (J_{DH}+J_{SH})\cdot a_{gnd}) \Bigg]^{0.25} \end{aligned} \quad (9)$$

Pickup et al. refers to T_{MRT} of Eq. (9) as OUT_MRT. This procedure supports the evaluation of insolation and radiation balance of a human body with f_p and E_{ff} obtained accurately in advance.

Computation of the Projected Area and Effective Radiation Area

To compute the radiation balance of a human body, the projected area and effective radiation area to the insolation direction must be determined in advance. The effective radiation area of a human body is an area contributing to radiant heat transfer with surrounding closed volume directly within the human body entire surface area, as derived by Fanger. Defining a sphere of radius r_m enclosing a human body as surrounding closed volume, and letting the projected area A_p of the human body to parallel rays from the spherical body of all directions, as presented in Fig. 2. The effective radiation area A_{eff} can be computed using the following equation:

$$A_{eff} = \frac{4}{\pi}\int_{\alpha=0}^{\alpha=\pi}\left(\int_{\beta=0}^{\beta=\frac{\pi}{2}}A_p\cos\beta d\beta\right)d\alpha \,. \quad (10)$$

The effective radiation area rate E_{ff} is defined as A_{eff}/A_{DU}. Here A_p is equal to the area of orthographic projection of human body surface parts that receive parallel rays to the plane of projection, and equivalent to the insolation transfer area for arbitrary solar positions. Accordingly, a sufficiently fine surface angle examined allows the projected area computation to direct projection to be included in the effective radiation area computation.

Although Ozeki (Ozeki et al., 1999) integrate only over a 1/4 sphere to obtain A_{eff}, the projected areas of each part in the upper hemisphere and the lower

hemisphere differ when the insolation transfer for each part that is examined. Therefore, computation is conducted by separating the upper and lower hemispheres as

$$A_{eff} = \frac{4}{\pi}\int_{\alpha=0}^{\alpha=\pi}\left(\int_{\beta=0}^{\beta=\frac{\pi}{2}} A_p \cos\beta d\beta\right)d\alpha = A_{eff}^{U} + A_{eff}^{D}$$

$$= \frac{2}{\pi}\int_{\alpha=0}^{\alpha=\pi}\left(\int_{\beta=0}^{\beta=\frac{\pi}{2}} A_p \cos\beta d\beta\right)d\alpha \qquad (11)$$

$$+ \frac{2}{\pi}\int_{\alpha=0}^{\alpha=\pi}\left(\int_{\beta=-\frac{\pi}{2}}^{\beta=0} A_p \cos\beta d\beta\right)d\alpha$$

where $E_{ff}^{U} = A_{eff}^{U} / A_{DU}$, $E_{ff}^{D} = A_{eff}^{D} / A_{DU}$.

This study used the virtual mannequin data presented by Ito (Ito et al., 2006). as a human body contour to determine the projected area. Their data comprise 44,974 surface elements (triangular) and 20 parts. Hair and sole parts were added to form 45,096 surface elements and 23 parts for the present analysis. Figure 3 depicts the human body contour used for analyses.

Projected area A_p was determined through image processing. The orthographic projection of each surface element of a human body was performed to a virtual screen normal to parallel rays from a viewpoint. The normal vector of a surface element was used; the surface of the opposite direction to the viewpoint was ignored. Surface elements facing the viewpoint were rearranged using Quicksort into descending order of distance from the viewpoint. Then they were drawn from the back to front. The overlapping of elements was examined, and triangular elements were filled with colors corresponding to human body parts. The virtual screen comprises 2,200 × 1,000 pixels, in which 1 pixel corresponds to 1mm^2. Figure 4 points to projected human bodies as an example. The pixel color information in this figure is counted and converted into the area of each part. A_p was determined with 1° step of azimuth and altitude.

Figure 5 depicts an equidistant projection distribution of A_p observed from the solar position direction, with a human body drawn facing south. This figure is applicable to a different direction by a rotating orientation. Actually A_p tends to be greater with

lower solar altitude, although it depends substantially on the orientation. Furthermore, A_p was about 0.15–0.2 m^2 when the solar altitude was 80°.

Figure 6 presents detailed A_p for each part (A_{pi}) (collective values shown for arms and legs). The overall value mostly shows good agreement with previously presented results. The figure suggests that the fraction for each part varies according to the incident condition of insolation.

Figure 7 presents a comparison of f_p computed from A_p and derived from Eq. (2).

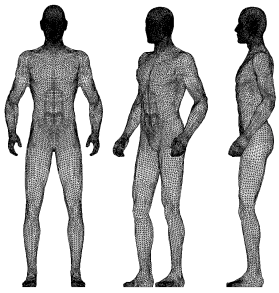

Area of whole body: 1.745 m^2
Height: 1.736 m, Volume: 0.064m^3
Mesh: 45,096, 23 parts
Min.: 0.469, max: 425.013 mm^2
face•hair•nose•mouth: 0.1475m^2
neck•ear: 0.0395 m^2,
chest:0.1903m^2,
back: 0.1266 m^2,
pelvis:0.2654m^2
shoulder•arm•hand (R):0.1837m^2
thigh•leg•foot (R): 0.3099 m^2
sole (R): 0.0141 m^2, symmetry

Fig. 3 Shape of virtual mannequin (α=0, -45, -90°).

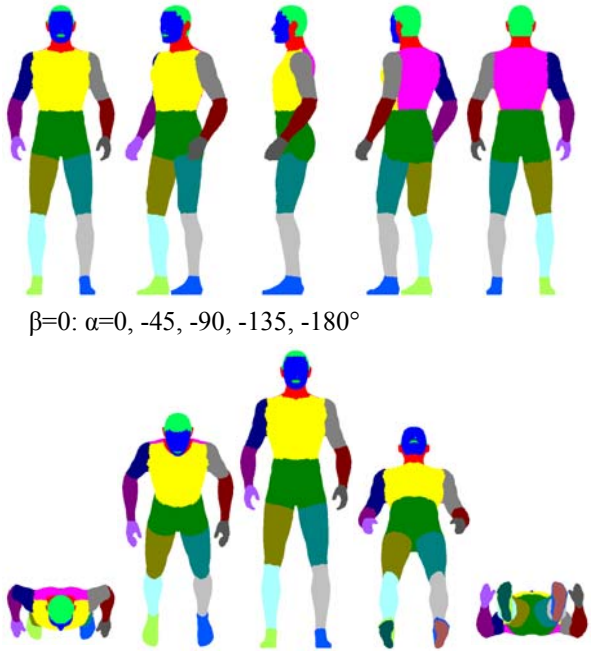

β=0: α=0, -45, -90, -135, -180°

α=0: β=90, 45, 0, -45, -90°

Fig. 4 Example of human body of orthographic projection.

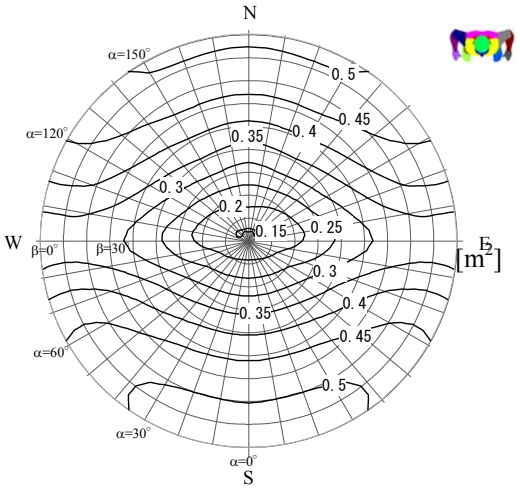

Human body: Facing South
Equidistant projection of Ap at each solar azimuth and altitude; outer and inner circles respectively represent azimuth and altitude (10° steps).

Fig. 5 Distribution of A_p (equidistant projection.)

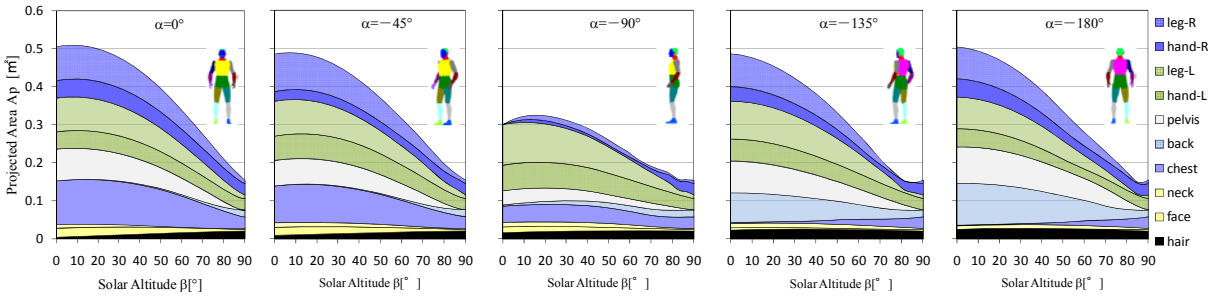

Fig. 6 Projected area of each part.

Pickup presented Eq. (2), which overestimates f_p compared with the present human body model. f_p averaged along the azimuth was comparable as azimuth –135. When the solar altitude alone was used for evaluating f_p, it was considered desirable to use an f_p value at α = 0, assuming a face-to-face position with the sun.

Next, Eq. (11) was applied to obtain the effective radiation area rate of E_{ff}. The integration angle was 1°. Because soles are usually contacting the ground surface, computations included a case in which soles were excluded. That result is presented in Table 1. Values for the upper and lower hemisphere were almost comparable, although the value for the lower hemisphere was slightly smaller when soles were excluded. The global effective radiation area rate was greater than the value of Fanger et al. by about 0.16. This is considered to be true because of posture differences: arms and legs of a human body were closed in the analyses conducted by Fanger et al. (See Note 2).

Figure 8 presents effective radiation area rate for each part(E_{ffi}). Values for the lower hemisphere were greater in the lower limbs (thighs, lower legs, and feet), although values for the upper hemisphere were greater on the head and chest. Moreover, the lower limbs occupy a great portion of the whole.

Computation of Insolation into a Human Body

OUT_MRT and insolation and radiation into a human body were computed using the projected area rate and effective radiation area rate obtained in the preceding chapter. Previous measurements (culmination) were used for exposure conditions such as insolation. Table 2 presents calculation conditions. Conditions related to a human body were set according to the previous references(Ozeki et al., 2004). Computation was conducted for cases of the whole human body and for each body part.

When the relationship between above-mentioned equations (1)-(7) is revalued every human body each part, the following equation (12) was obtained using f_{pi} and E_{ffi} for each part i. In this equation, the value which differs for insolation absorption ratio and long wavelength emissivity in each human body part can be set.

Figure 9 presents computation results of OUT_MRT, OT, and the clothes surface temperature.

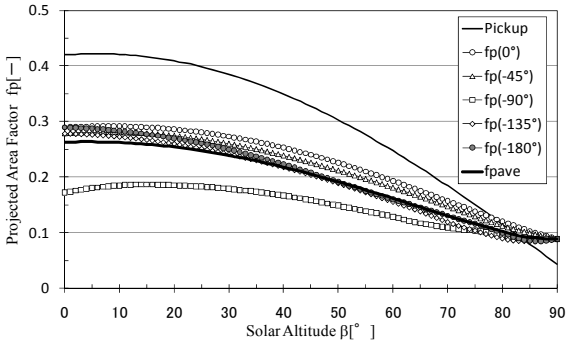

Fig. 7 Comparison of projected area factor f_p.

Table 1 Effective radiation area factor

	Include sole	No sole	Fanger et al.
A_{DU} [m²]	1.7453	1.7453	1.74
A_{eff} [m²]	1.5467	1.5182	1.262
E_{ff} [–]	0.8862	0.8699	0.723±0.013
E_{ff}^{U} [–]	0.4431	0.4431	0.3615
E_{ff}^{D} [–]	0.4431	0.4268	0.3615

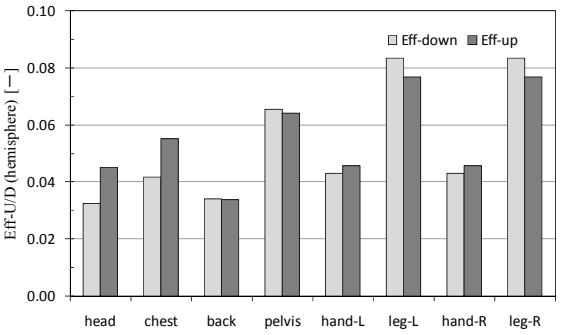

Fig. 8 Effective radiation area factor of each part (hemisphere).

$$OUT\_MRT_i = \left[\frac{E_{ff\,i}^{U}}{\sigma E_{ff\,i}} J_a + \frac{E_{ff\,i}^{D}}{\sigma E_{ff\,i}} J_g + \frac{f_{p\,i}(1-a_{body\,i})}{\sigma E_{ff\,i}} J_{DN} + \frac{E_{ff\,i}^{U}}{\sigma E_{ff\,i}}(1-a_{body\,i}) J_{SH} + \frac{E_{ff\,i}^{D}}{\sigma E_{ff\,i}}(1-a_{body\,i})(J_{DH}+J_{SH})\cdot a_{gnd} \right]^{0.25} \quad (12)$$

Table 2 Calculation conditions

Measurement place: Ordinary pavement, Shinagawa, Tokyo (Sakai et al., 2007)
Date: 11:30, July 29, 2005, Solar location: β=73.9°, α=0°
Solar radiation:
Global solar radiation: 877.68 W/m^2,
Direct (J_{DN}): 745.48 W/m^2, Diffuse (J_{SH}): 161.98 W/m^2,
Long wave radiation:
Atmospheric (J_a): 425.84 W/m^2,
Ground surface (J_g): 577.68W/m^2, Ground albedo: 0.07[-],
Air temp.: 32°C, RH: 50%, Wind velocity: 1.6 m/s,
Globe Temp.: 44°C
Manikin: South direction, emissivity of body: 0.9,
Metabolic rate: 1.0 met
Albedo of body surface: whole body=0.4, hair=0.1,
face•neck•arm•hand=0.3, chest•back=0.8, other=0.6[-]
Clothes: whole body=0.6, hair•face•neck•arm•hand=0,
other=0.6 clo
Projection area factor: Fig. 7(α=0), E_{ff}: Table 1 (no sole)
Temp. of cloth surface l: calculated from PMV.

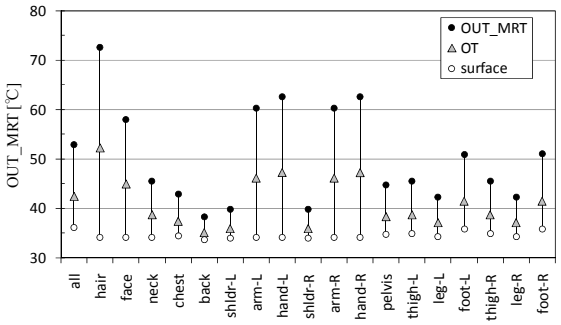

Fig. 9 OUT_MRT of each part.

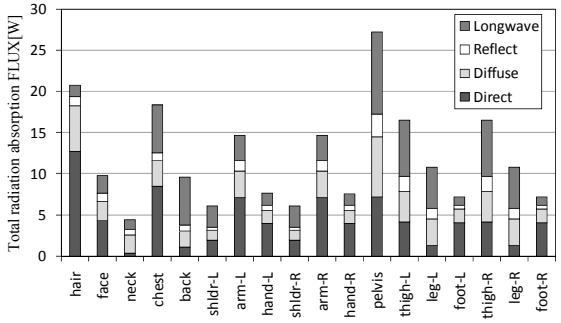

Fig. 10 Total radiation absorption of each part.

Overall OUT_MRT and OT were about 53 °C and 42.5 °C, respectively. Because the actual measurement of globe temperature was 44 °C, the computed values were considered mostly appropriate. High OUT_MRT$_i$ was observed at parts that received insolation, such as hair and hands; that of hair was 73 °C, which was higher than those of other parts because the solar reflectance was set as 0.1.

Figure 10 shows the global radiation absorbed by each part of a human body. Computation of long wavelength absorption with Eq. (5) necessitates quantification of the human body surface temperature, which was acquired from PMV computation with the mean radiant temperature assumed as OUT_MRT. Total absorption by the whole human body was 263.5 W (151.0 W/m^2). Absorption at the waist, hair, and chest were greater than at other parts.

CONCLUSION

A procedure for computing incident solar radiation to each human body part, applicable to a 65-division thermoregulation numerical human body model, was constructed in this study, based on the methods of Ozeki et al. and Pickup et al. Then incident insolation into each part of a human body was evaluated. The obtained results are summarized as follows:

- The projected area for each human body part of standing posture was determined accurately using image processing. Furthermore, effective radiation area rates for each part were computed.

- Computation of insolation and radiation into human body parts was implemented using projected area rate and the effective radiation area rate.

This line of research will be extended in the future to encompass evaluation of thermal environment such as a high reflective pavement surface, a space under a membrane roof, etc., and to analyses of a thermal reaction model for the human body.

NOTE

1) The original paper of Pickup (Pickup et al., 1999) employs the global effective radiation area rate of Fanger, as effective radiation area in Eqs. (3) and (4). For that reason, T_{MRT} is derived from the following equation (a), which differs in the coefficient of the last term of the right-hand-side from Eq. (9).

$$T_{MRT} = \left[\frac{1}{2\sigma}(J_a + J_g) + \frac{f_p(1-a_{body})}{\sigma E_{ff}} J_{DN} + \frac{(1-a_{body})}{\sigma}(J_{SH} + (J_{DH} + J_{SH}) \cdot a_{gnd}) \right]^{0.25} \quad \text{(a)}$$

It is considered desirable that evaluation of the effective radiation area rate be identical between diffuse sky radiation and atmospheric radiation, and between reflected solar radiation and ground surface radiation. Therefore in this paper, the effective radiation area rate over the upper and lower hemispheres was applied, respectively, to the evaluation of Eqs. (3) and (4).

2) A human body of standing posture was generated using 3DCG software, and E_{ff} computation was conducted with the opening of arms and legs varied. The configuration differs from that in this paper. In fact, E_{ff} was 0.839 in the same opening as this paper and 0.783 with arms and legs closed. Consequently, results show that the effects of contour and posture were considerable.

REFERENCES

Fanger P.O., Angelius O. and Jensen P.K. (1970). Radiation Data for the Human Body, ASHRAE Transactions, Vol.76-II, pp.338-373.

Ito K, Hotta T (2006). Development of Virtual Manikins and Its Grid Library for CFD Analysis, Air-Conditioning and Sanitary Engineers of Japan, (113):27-33. (in Japanese)

Ito, Y et al. 1953. The Heating Value of Human Body by Solar Radiation, University of Osaka City, (24):271-272. (in Japanese)

Kondo Y, Ogasawara T, Kanamori H (2009). Field Measurements and Heat Budget Analysis on Sensible Heat Flux From Pavement, Journal of environmental engineering, 73(628):791-797. (in Japanese)

Michikawauchi R, Yamada N, Saitoh T (2004). Study of Measurement of and Simulation of Thermal Environment in Urban Street Canyon in Tokyo and Sendai, Proceedings of JSES/JWEA Joint Conference, 37-40. (in Japanese)

Miyamoto S, Tomita A, Horikoshi T (1998). The Projected Area of The Human Body and Human Shape Model at The Standing, Summaries of Technical Papers of Annual Meeting Architectural Institute of Japan,373-374. (in Japanese)

Nakajima R, Yoshida H, Umemiya N, Majima M (2005). Evaluation of Thermal Comfort in Different Configurations of the Street in Summers, Summaries of Technical Papers of Annual Meeting Architectural Institute of Japan,647-648. (in Japanese)

Ozeki Y, Hiramatsu T, Tamabe S (2004). Comparison of Skin Surface Temperatures Between Subjective Experiments and Numerical Predictions by Using A Modified 65MN Thermoregulation Model Under Solar Radiation, Journal of Environmental Engineering,(581): 29-36. (in Japanese)

Ozeki Y, Konishi M, Narita C, Tanabe S (1999). Evaluation on Effective Radiation Area of Human Body Calculated by A Numerical Simulation, Journal of Architecture Planning and Environmental Engineering. Transactions of AIJ ,(525):45-51. (in Japanese)

Pickup J, Dear R (1999). An Outdoor Thermal Comfort Index (OUT_SET*) - Part I – The Model and its Assumptions, Proc. of the 15th Int. Congress of Biometeorology and Int. Conference on Urban Climatology, pp.ICB9.4.1-6.

Sakai K, Tsuyuki T, Murata Y, Matsuo Y, Miki K Murase T (2007). Thermal environment measurement of the pavement which conducted high reflection paint, Journal of Japan Solar Energy Society, 33(5): 43-50. (in Japanese)

Tsuchikawa T, Kobayashi Y, Horikoshi T, Miwa E Kurazumi Y, Hirayama K (1988). The Effective Radiation Area of The Human Body and Configuration Factors Between The Human Body and Rectangular Planes And Measured by The Photographic Method, Journal of Architecture, Planning and Environmental Eengineering. Transactions of AIJ, (388): 48-59. (in Japanese)

Underwood C.R. and Ward E.J. (1966). The Solar Radiation Area of Man, ERGONOMICS, Vol.9, No.2, pp.155-168.

Watanabe S, Koganezawa S, Horikoshi T Tomita A (2009). Measurement of solar radiation absorptance of different clothing fabric for outdoor thermal comfort study, Journal of Environmental Engineering, 45(4): 121-129. (in Japanese)

Yamada N, Saito T (2002). Study on Thermal Environment Validation Affected by Solar Radiation in Urban Street Canyon, Journal of Japan Solar Energy Society, 28(5): 65-70. (in Japanese)

Yoshino T, Oyakawa A, Hoyano A (2008). The heat radiation environment in summer under a membrane roof of platform canopies at station, Journal of Membrane Structures Association of Japan, (22) :55-63. (in Japanese)